

Nuclear Electric Quadrupole Moment of Na^{23} by the Atomic Beam Resonance Method*†‡M. L. PERL,§ I. I. RABI, AND B. SENITZKY
Columbia University, New York, New York

(Received January 27, 1955)

The hyperfine structure of the $n=3$ $^2P_{1/2}$ and $^2P_{3/2}$ excited atomic states of Na^{23} have been investigated using a modification of the atomic beam resonance method. The C region is illuminated with resonance radiation from a sodium discharge lamp which brings some of the atoms into the excited levels where they have lifetimes of the order of 10^{-8} sec. The application of an rf field of an appropriate frequency causes transitions among the excited state hyperfine levels and "scrambles" the populations of these levels. Since the atoms are essentially "tagged" by the deflection which they have undergone in the A field, this "scrambling" will cause a change in the refocused intensity at the detector.

Measurements of the hyperfine structure at weak fields give the values: $a_3=94.45\pm 0.5$ Mc/sec for the $^3P_{1/2}$ state; $a_3=19.06\pm 0.36$ Mc/sec for the $^3P_{3/2}$ state; and $b=+2.58\pm 0.3$ Mc/sec or $b=-21.64\pm 0.7$ Mc/sec for the $^3P_{3/2}$ state. The strong-field spectrum of the $^3P_{3/2}$ state strongly indicates that the correct value of b is $+2.58\pm 0.3$ Mc/sec. The possible values of Q are $+0.100\pm 0.011\times 10^{-24}$ cm for $b=+2.58$ Mc/sec, or $-0.836\pm 0.028\times 10^{-24}$ cm for $b=-21.64$ Mc/sec.

1. INTRODUCTION

a. Purpose of the Experiment

THE purpose of this paper is to describe in more detail a new method¹ for studying the hyperfine structure of the excited states of atoms by the atomic beam resonance method. Our initial purpose in these experiments has been to measure the nuclear electric quadrupole moment of the alkali atoms. This paper gives the results on Na^{23} which was the first alkali to be studied. The nuclear quadrupole interaction must be measured in an excited state of the alkalis because the ground state is a $^2S_{1/2}$ which has no quadrupole interaction. The lowest excited state with a quadrupole interaction is the $^2P_{1/2}$ state in the same n level. The hyperfine structure in this state in the alkalis is too small to be measured optically with sufficient accuracy to determine the quadrupole interaction. In higher excited states the hyperfine structure is even smaller.

The nuclear electric quadrupole moment of Na^{23} is of particular interest to nuclear shell theory. The experimental spin of $\frac{3}{2}$ disagrees with the simplest shell model prediction of $5/2$. If a $(d_{3/2})^3$ shell model assignment of the protons is used to obtain the correct spin, then the quadrupole moment will be zero. The quadrupole moment was first shown not to be zero by a molecular beam study of the hyperfine structure due to Na^{23} in molecules.² More recently, Sagalyn³ has used a new double-resonance optical method to examine the hyperfine structure of the $^3P_{3/2}$ state of Na^{23} , and has obtained an approximate value of the nuclear quadru-

pole moment. In our experiment, we have been able to measure the hyperfine structure of the $^3P_{1/2}$ and $^3P_{3/2}$ states, and therefore the nuclear quadrupole moment, more precisely.

The nuclear quadrupole moments of Na^{23} and the other alkalis are also of interest as an aid in surmising the electronic wave functions of the alkali halide molecules. A great deal of information on the alkali quadrupole interaction in these relatively simple molecules has been accumulated with molecular beam electric and magnetic resonance techniques and with high-temperature microwave spectroscopy. Although these data can be used to evaluate the ratio of the quadrupole moments of the isotopes of the same element, the evaluation of the magnitude of the quadrupole moment requires an accurate knowledge of the molecular wave functions, which is not available at present. Conversely, to utilize the quadrupole moment interactions to gain insight into the nature of the molecular wave functions requires a knowledge of the nuclear quadrupole moment. These atomic experiments which establish the nuclear quadrupole moment through conventional atomic calculations can therefore be used to discuss the molecular wave functions.

Another general use of the atomic beam resonance method as applied to excited states is that it provides a way of investigating atomic wave functions. For example, in this experiment we have relatively precise measurements of the magnetic interaction constants in the $^2P_{1/2}$ and $^2P_{3/2}$ states to compare with the calculation of those constants from the fine structure separation. This provides a test of the theory of atomic hyperfine structure in the case of a single valence electron. By extending this method to examine more excited states, the theory of atomic hyperfine structure could be examined further. Finally it should be noted that the width of the resonance lines is a direct measure of the lifetime of the excited state.

In the past, the atomic and molecular beam resonance method has been limited to the study of the hyperfine

* A brief account of this experiment was given previously; Perl, Rabi, and Senitzky, *Phys. Rev.* **97**, 838 (1955).

† Submitted by Martin L. Perl in partial fulfillment of the requirements for the degree of Doctor of Philosophy in the Faculty of Pure Science at Columbia University.

‡ This work was supported in part by the Office of Naval Research.

§ Present address: Physics Department, University of Michigan, Ann Arbor, Michigan.

¹ I. I. Rabi, *Phys. Rev.* **87**, 379 (1952).

² Kusch, Millman, and Rabi, *Phys. Rev.* **55**, 1176 (1939).

³ P. L. Sagalyn, *Phys. Rev.* **94**, 885 (1954).

structure of ground or metastable energy levels because the natural lifetime of excited atomic states is 10^{-7} to 10^{-10} sec. In the conventional beam method the lifetime of the state under study must be greater than the time required for the particles in the beam to traverse the apparatus which is 0.001 to 1.0 sec. Traversal times of this magnitude are required because the particles with thermal velocities must travel a distance of the order of one meter.

Since the hyperfine structure of excited atomic states have long been studied by means of optical spectroscopy, it is proper that the value of applying the atomic beam resonance method to excited states be discussed. The application of the atomic beam resonance method to excited states makes possible the measurement of hyperfine separations which are too small to be measured by optical spectroscopy. Also with this method hyperfine separations can be measured to much greater accuracy. Indeed, it will be seen from this paper that the limitation on the accuracy of the hyperfine excited state measurements by the atomic beam resonance method is not the apparatus resolution, but the large width of the resonance curves due to the short lifetime of the excited state. This natural line width is of the order of 100 times greater than the line width produced by the apparatus resolution. The range of level separations which can be measured is limited by the availability of practical electromagnetic oscillators, but with present oscillators it is possible to study all hyperfine level separations. Some of the smaller fine structure separations are also within range, such as in the 3^2D states in Na^{23} .

b. Outline of the Experimental Method

As in the usual atomic beam experiment, there are two deflecting magnets *A* and *B*, Fig. 1, and a region *C* in which the atom may be induced to undergo a transition by a radio-frequency field in a homogeneous

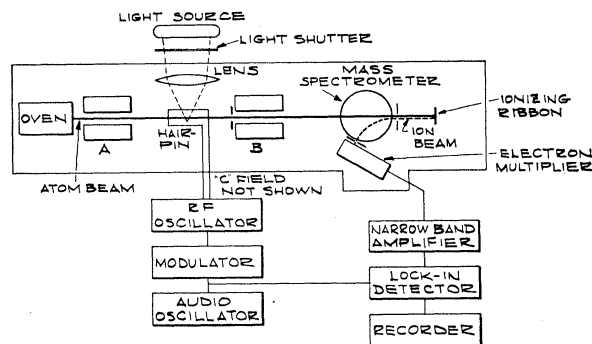


FIG. 1. Schematic drawing of the apparatus. The light source is shown on the side of the apparatus for clarity, but it actually lies above the apparatus. The *C* magnet, which produces a homogeneous field in the "hairpin," is also not shown for clarity. The six external boxes which represent the major electronic components do not indicate the physical position of the components.

static magnetic field of the desired strength. In ground state atomic beam experiments, the atom traverses the apparatus in the states in which it is being studied. If in the *C* field the atom makes a transition from the state (1) to the state (2), this means that the atom traverses the *A* field in state (1) and *B* field in state (2). In our experiment, the atom while in the *C* field is subjected to optical radiation from a sodium discharge lamp which raises the atom to an excited state, principally the $3^2P_{3/2}$ or $3^2P_{1/2}$ state. The lifetimes of these excited states are about 10^{-8} sec, which is much less than the time required for the atom to traverse the *C* field, so that the atoms all decay to the ground state before leaving the *C* field. In decaying the atom may end up in a magnetic hyperfine ground state which is different from its initial magnetic hyperfine ground state.

In our experiment, the *A* and *B* deflecting fields are strong fields so that the deflection of the atom depends only on the value of m_J . Since the ground state is an $2S_{1/2}$ state, the value of m_J is $+\frac{1}{2}$ or $-\frac{1}{2}$ as shown in Fig. 2. The *A* and *B* magnets are arranged so that the gradients of their fields point in the same direction. For an atom to be refocused, that is to hit the detector wire, the deflections in the two fields must be of opposite sign. Therefore for an atom to be refocused the m_J must change in the *C* field. If the atom, after being optically excited, decays to a ground magnetic hyperfine state with an m_J value different from the m_J value of its initial magnetic hyperfine ground state, then the atom is refocused. The signal produced at the detector by the portion of the beam which is refocused by optical radiation is referred to in this paper as the light effect.

To study the hyperfine structure of the excited state, the radiofrequency magnetic field is applied to the illuminated portion of the beam. Just as in ground state work, the rf field produces rf transitions between two hyperfine levels if the frequency of the rf corresponds to the frequency separation of the two hyperfine levels. If the rf is of the correct frequency, some of the excited atoms will change their hyperfine excited states before decaying. Since the atoms are essentially "tagged" by the deflections which they have undergone in the *A* field, this rearrangement in the excited state produces a change in the intensity of the refocused beam. The signal produced at the detector by the change in refocused beam induced by an excited state rf transition is referred to in this paper as the excited state rf effect.

By sweeping the frequency of the rf across the hyperfine structure of the excited state, the rf spectra of the excited state are obtained. These rf spectra are then used, as with the ground state rf spectra, to evaluate the various nuclear interaction constants. By varying the static magnetic field, the Zeeman and Paschen-Back effects of the excited state can be studied.

2. THEORY OF THE EXPERIMENT

a. Theory of the Hyperfine Structure

The hyperfine structure of the $3^2P_{3/2}$ state of Na²³ is shown in Fig. 2. At zero field the $3^2P_{3/2}$ state has four F levels each having a degeneracy of $2F+1$. The separations between these levels at zero magnetic field are:

$$\begin{aligned} 3a_{3/2} + b & \text{ for } F=3 \text{ to } F=2, \\ 2a_{3/2} - b & \text{ for } F=2 \text{ to } F=1, \\ a_{3/2} - b & \text{ for } F=1 \text{ to } F=0, \end{aligned} \quad (1)$$

where $a_{3/2}$ is the magnetic dipole interaction constant and b is the electric quadrupole interaction constant. These separations are the essential results of this experiment, and are determined by making $\Delta F = \pm 1$ rf transitions at near-zero magnetic field. At near-zero field each transition will consist of a number of almost superimposed Zeeman transitions with $\Delta m_F = \pm 1$ or $\Delta m_F = 0$, depending on whether the rf magnetic field is perpendicular or parallel to the static magnetic field.

The strong field spectrum of the $3^2P_{3/2}$ state is easily obtained because the small value of $a_{3/2}$ enables a field of the order of 50 gauss to almost completely decouple I and J . The strong field level pattern is also shown in Fig. 2. The selection rules in this case are $\Delta m_J = \pm 1$ and $\Delta m_I = 0$ for the oscillating magnetic field perpendicular to the static magnetic field.

The $3^2P_{3/2}$ state of Na²³ has a hyperfine structure similar to the $3^2S_{3/2}$ state with about a tenth of the magnetic dipole interaction constant, Fig. 2. At small magnetic fields the transition of interest is $F=2$ to $F=1$, with a separation of $2a_{3/2}$.

b. Theory of the Effect of Optical Radiation on the Beam

In this section, we will discuss the effect of the optical radiation on the beam, that is, the theory of the light effect. Since the general calculation of the light effect is complicated, we shall first describe the process by following a typical atom as it traverses the apparatus. For definitiveness we will use Na²³ under the conditions of the present experiment.

We first recall that the A and B fields are strong fields and that an atom must change its m_J value in the C region in order to be refocused. For simplicity we consider only those atoms which are excited to the $3^2P_{3/2}$ state in a weak field. We will take as an example an atom traversing the A field in the state $m_J = \frac{1}{2}$, $m_I = \frac{1}{2}$. Upon entering the C field, the state of this atom is then designated by the quantum numbers, $F=2$, $m_F=1$, which we write as (2,1) for brevity. The resonance radiation which excites the beam is unpolarized so that the selection rules on the optical transition are $\Delta F = 0, \pm 1$ and $\Delta m_F = 0, \pm 1$. Since the atom is initially in the ground (2,1) state, it may be raised to any of the

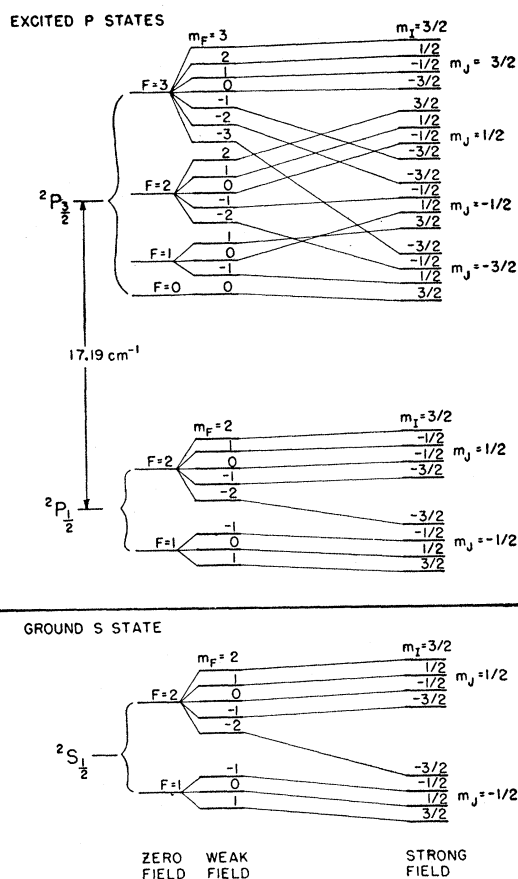


FIG. 2. A diagram of the ground $3^2S_{3/2}$ state and excited $3^2P_{3/2}$ and $3^2P_{1/2}$ states of Na²³. The separation of the $3^2S_{3/2}$ and $3^2P_{1/2}$ states is 5890 Å. The separations of the levels are not drawn to scale. The magnitudes of the magnetic fields corresponding to the weak and strong field patterns of each fine-structure state depend on the strength of the I -to- J coupling in that fine-structure state. Thus a field can be sufficiently strong to give a strong-field pattern in the excited states but not give a strong-field pattern in the ground state.

following excited states: (2,2), (2,1), (2,0), (1,1), or (1,0). Before the atom leaves the C field it will decay to the ground state. The selection rules for the optical decay are also $\Delta F = 0, \pm 1$ and $\Delta m_F = 0, \pm 1$. Thus the excited (2,2) state can decay to the ground (2,2), (2,1), or (1,1) states. Indeed, let us suppose that the atom initially in the ground (2,1) state was excited to the (2,2) state. If it decays to the (2,2) or (2,1) ground states it will have the quantum number $m_J = \frac{1}{2}$ in the B field. Since it had the same m_J value in the A field, it will not be refocused. But it can also decay to the (1,1) ground state. In this case it has the quantum number $m_J = -\frac{1}{2}$ in the B field. Since the m_J value has changed the atom is refocused.

To calculate the probability that the atom initially in the (2,1) ground state is refocused, all the other possible paths must be considered. For example, it might have been raised to the excited (1,1) state and could then have decayed to the ground (2,2), (2,1),

(2,0), (1,1), or (1,0) states. Actually the quantitative probability amplitudes must be used for a systematic calculation of the processes involved. It should be pointed out that atoms which go through reversed excitation and decay paths do not cancel each other. Thus, if atom (a) goes from the ground (2,1) state through the excited (2,2) state to the ground (1,1) state, and if atom (b) goes from the ground (1,1) state through the excited (2,2) state to the ground (2,1) state, both atoms are refocused.

The magnitude of the light effect depends on the probability that an atom is excited and the probability that an excited atom changes its m_J value when it decays. The probability of excitation depends on the intensity of the optical radiation and the time that the atom spends in the optical radiation field, both of which are experimental parameters. The probability that an excited atom changes its m_J value is a theoretical calculation of the kind of processes considered in the last two paragraphs, and depends on the polarization of the exciting radiation, the static magnetic field and the hyperfine structure of the state. The last two parameters enter the calculation because of the quantum mechanical interference of hyperfine levels which have widths of the order of magnitudes of their separations. A general equation for these processes was derived from the work of Breit⁴ on the effect of this interference on the polarization of scattered resonance radiation. The general equation depends on the separations of the excited state hyperfine levels since the interference between levels decreases as the separation of the levels increases. Since the separations are complicated functions of the static magnetic field, the general calculation of the light effect variation with magnetic field is tedious. The general theory and a few simplified calculations are outlined in Appendix 1.

In this type of experiment which has as its object the measurement of the hyperfine separations of the excited state, the theoretical calculation of light effect is of no direct interest. The calculations are of use only as a means of gaining insight into the optical processes occurring in the experiment. It should be pointed out that in principle the variation of light effect with the static magnetic field can be used to study the hyperfine structure. This is analogous to the work of Larrick⁵ and of Ellet and Heydenburg.⁶ As in their work, this cannot be done in practice because the measurements are not sufficiently precise and the labor involved in determining both $a_{\frac{1}{2}}$ and b is prohibitive.

c. Theory of the Combined Effect of rf and Optical Radiation

In this section, the effect of the radio-frequency field on the beam in the presence of the optical radiation will

be discussed. This excited state rf effect is to be distinguished from the ground state rf effect, where the latter term refers to the signal produced at the detector by rf transitions in the ground state. The theory of the excited state rf effect is more complicated than the theory of the ground state rf effect because of the properties of the excited state and the method of the experiment. Therefore the theory of the ground state rf effect will be outlined in the next paragraph as a basis for discussing the excited state rf effect.

In our apparatus a ground state rf transition must be between states of opposite m_J values to refocus the atom. For example the rf transition (2,2) to (1,1) produces a refocused beam but the rf transition (2,2) to (2,1) does not. There is an optimum value for the magnitude of the rf magnetic field at which 77 percent of the atoms in the two levels are refocused and the resonance width is the reciprocal of the time that the atom spends in the rf field.⁷ In our experiment, this width would be about 50 kc/sec. At higher magnitudes of the rf field the amount refocused decreases to some extent, and the width of the rf resonance increases.

We shall begin the discussion of the excited state rf effect with a simple example. We will consider an atom with a nuclear spin of zero, with a ground state of $J=\frac{1}{2}$, and with an excited state of $J=\frac{1}{2}$, in a magnetic field which separates the Zeeman levels as shown in Fig. 3. We will consider an atom originally in the ground $m_J=+\frac{1}{2}$ state so that the original populations are 1 in the ground $m=+\frac{1}{2}$ state and 0 in the ground $m_J=-\frac{1}{2}$ state. We illuminate the atom with isotropic optical radiation so that the relative transition probabilities for both excitation and decay are the same and are given in Fig. 3. If one uses these transition probabilities, the population of the excited $m_J=+\frac{1}{2}$ state is $\frac{1}{3}$ and the population of the excited $m_J=-\frac{1}{2}$ state is $\frac{2}{3}$. When the atom decays the final populations are $\frac{5}{9}$ in the $m_J=+\frac{1}{2}$ ground state and $\frac{4}{9}$ in the $m_J=-\frac{1}{2}$ ground state. Therefore the probability is $\frac{4}{9}$ that when the atom is excited it changes its m_J value, and this gives a ratio of the light effect to the total beam of $\frac{4}{9}$, if all atoms are optically excited once.

To measure the separation between the two excited Zeeman levels, an rf field with a frequency equal to this separation is applied. Let us suppose that the probability of an excited atom making an rf transition in the excited state before decaying is $\frac{1}{2}$. Then $\frac{1}{2}$ of the population of the excited $m_J=+\frac{1}{2}$ state goes to the excited $m_J=-\frac{1}{2}$ state and $\frac{1}{2}$ of the population of the excited $m_J=+\frac{1}{2}$ state goes to the excited $m_J=+\frac{1}{2}$ state. Therefore the rf changes the excited state population to $\frac{1}{2}$ in either excited state. Now when the atom decays the population of the final $m_J=+\frac{1}{2}$ ground state is $\frac{1}{2}$ and the final $m_J=-\frac{1}{2}$ ground state is also $\frac{1}{2}$. The ratio of refocused atoms to total beam is now $\frac{1}{2}$ if all atoms are optically excited once. The fractional in-

⁴ G. Breit, *Revs. Modern Phys.* **5**, 91 (1933).

⁵ L. Larrick, *Phys. Rev.* **46**, 581 (1934).

⁶ A. Ellet and N. P. Heydenburg, *Phys. Rev.* **46**, 583 (1934).

⁷ H. C. Torrey, *Phys. Rev.* **59**, 293 (1941).

crease in refocused beam is $\frac{1}{3}$, and this increase is the excited state rf effect.

If atoms are present in the beam which are originally in the $m_J = -\frac{1}{2}$ ground state, they can be followed through the excitation and rf transition in the same manner. Each atom is "tagged" by the deflection which it underwent in the A field, and therefore the atom "remembers" its original m_J state. In the simple case being considered here, the excited state rf effect is the same for atoms originally in the $m_J = +\frac{1}{2}$ state or atoms originally in the $m_J = -\frac{1}{2}$ state. The total excited state rf effect is simply the sum of the excited state rf effects produced by the atoms from each initial state.

While the example which was considered above is a very simple case, it illustrates the essential mechanism of the excited state rf effect. The effect does not depend on changing the relative populations of the final ground states. The effect depends on altering the way in which the atoms from each initial ground state distribute themselves when decaying back to the ground state from the excited states in which the rf transition took place. In the example given above, the excited state rf effect was an increase in the number of refocused atoms, but in general one might expect to find cases in which the rf excited state transition leads to a decrease in the refocused beam. In our work we have always found that the excited state rf effect is an increase in the refocused beam.

To calculate the amount of rf excited state effect for an actual transition it is necessary to consider in detail the probability amplitudes for the various rf and optical transitions which are involved. The calculation is complicated by the presence of quantum mechanical interference terms in the excited state and rf perturbation of the excited state energy levels. The interference terms are similar to those present in the theory of the light effect and result in the intensity of the excited state rf effect being dependent on the separations of the excited hyperfine levels, the widths of these levels, and the magnitude of the rf magnetic field. The general theory for the cases of the excited state rf effect in zero static magnetic field has been worked out by Serber.⁸ The theory for the simple case of strong static magnetic field, weak rf magnetic field, and neglect of interference terms is given in Appendix 2. The intermediate case of static magnetic field and rf magnetic field of the same order of magnitude is quite complicated and has not been worked out in detail. As in the theory of the light effect, the theory of the excited state rf effect is of use primarily for understanding the mechanism of the experiment and there is no need for exact calculation of the excited state rf effects. Therefore in the next few paragraphs we will discuss the qualitative conclusions which can be drawn from the theory of the excited state rf effect.

The first conclusion about the excited state rf effect

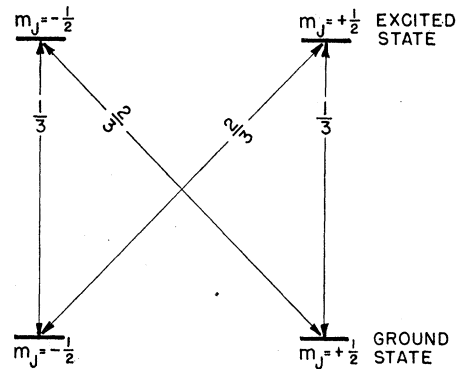


FIG. 3. The energy levels of a hypothetical atom with zero nuclear spin, with a ground state J of $\frac{1}{2}$, and with an excited state J of $\frac{3}{2}$, in a magnetic field. The numbers on the diagonal arrows are the relative transition probabilities for excitation by isotropic radiation or for decay. This example is used to illustrate the excited state rf effect.

is that the intensity, unlike the ground state rf effect, depends on a complicated process and can vary considerably for different transitions even if the rf magnetic field and the rf transition probability are the same. In general, it is also to be expected that indirectness of the excited state rf effect will lead to smaller signals than are usual in the ground state effect. Thus, in the simple example given above, the rf excited state effect was only $\frac{1}{3}$ of the total refocused beam although the probability of an excited state rf transition was taken as $\frac{1}{2}$. In more complicated optical spectra, the ratio of the excited state rf effect to the light effect will be much smaller.

There are no observational selection rules on the excited state rf transitions, and all transitions which obey the magnetic dipole selection rules can in principle be observed in our apparatus. Of course, some of the resulting excited state rf effects may be quite weak and difficult to observe, unless the signal-to-noise ratio is high.

The most important way in which excited state rf resonances differ from ground state rf resonances is that the former are much broader than the latter. The width of the excited state resonance is equal to twice the width of the excited state energy levels. For the $3^2P_{3/2}$ state of Na^{23} the lifetime is 1.7×10^{-8} sec, giving an energy level width of about 10 Mc/sec, and a width for the rf resonance at half intensity of about 20 Mc/sec. This is 400 times the width due to apparatus resolution. Therefore the measurement of excited state hyperfine separations will be relatively less accurate than the measurement of ground state hyperfine transitions. This is a result of a property of the excited state and not of the method. To get high accuracy it will be necessary to attain high signal-to-noise ratios and to understand the line shape.

A high signal-to-noise ratio can be attained by strong excited state rf effects, but unfortunately the excited state itself makes this difficult to attain. The proba-

⁸ R. Serber (to be published).

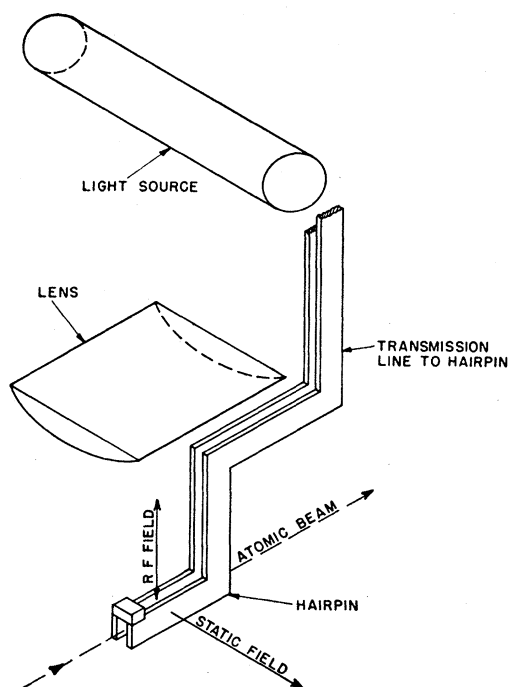


FIG. 4. A diagram of the relative positions of the static and rf fields, the light source, and the atomic beam. The static magnetic field, the rf magnetic field, and the atomic beam are mutually perpendicular. The light source lies above the hairpin so that the light beam is propagated parallel to the direction of the rf field. The lens focuses the light beam into the hairpin.

bility of inducing an excited state rf transition is proportional to the lifetime of the excited state, while the probability of inducing a ground state rf transition is proportional to the time that the atom spends in the rf field, if the magnitude of the rf field is less than the optimum magnitude. The ratio of the lifetime of the excited state to the time the atom spends in the rf field is about $1/1000$, for our apparatus. Therefore to achieve the same magnitude of rf transition probability in the excited states as in the ground state, the rf field used for the excited state transition must be about 1000 times larger than the field used in the ground state transition. It should be recalled that high rf transition probability in the excited state still does not lead to high excited state rf effects because the production of the effect is an indirect process. Therefore it is necessary to use rf magnetic fields of the order of magnitude of a gauss or more to get easily observable excited rf effects. Summarizing this discussion of the rf excited state effect, one may expect to find that the excited state resonances are broader and much less intense than ground state resonances and that the intensity of different excited state rf transitions will vary widely.

In this experiment, we have used unpolarized light and all the hyperfine ground states. It is possible to design an apparatus in which various types of polarized light are used and in which only certain hyper-

fine ground states enter the C field region. Only a few excited hyperfine levels would then be involved and the rf transition would have a much greater net effect on the final disposition of the atoms after decay. This would lead to a substantial improvement in the ratio of excited state rf effect to total beam. By exciting to only a single excited state the rf excited state transition can also be directly identified. Finally it would be easier to apply the theory of the excited state rf effect if the number of excited levels is restricted. Therefore with a suitably designed apparatus the problems now associated with the excited state rf effect can be considerably reduced.

3. DESCRIPTION OF THE APPARATUS

a. General Description

The apparatus shown schematically in Fig. 1 was originally designed and built for a ground state experiment and had to be adapted to the excited state experiment without drastic modifications. For this reason it should not be taken as a model for future excited state experiments. The oven, magnets, collimating system, and vacuum system were of the usual design.⁹ The deflecting A and B magnets were iron magnets with a ratio of gradient to field of 3. For sodium the A and B fields were about 10 000 and 8000 gauss respectively, the deflection therefore depending only on the m_J of the atom. The oven slit was 0.04 mm wide, the collimator was 0.1 mm wide, and the cross section of the beam at the detector was 0.3 mm wide by 6 mm high. The s_α of either inhomogeneous field was 2.7 mm.

The C field magnet had a $\frac{1}{2}$ -in. gap which contained the "hairpin" which applied the radiofrequency magnetic field to the beam. In Fig. 4, the atomic beam is represented by the dashed line, and the oscillating magnetic field, which is perpendicular to the beam, is represented by the arrow marked "rf." The static magnetic field which is perpendicular to both the atomic beam and the rf magnetic field, is represented by the arrow marked "static." This type of hairpin was used to attain a high ratio of rf magnetic field to rf current in the hairpin while having a large opening for the light source to illuminate the beam. The ratio of the average rf magnetic field seen by the beam to the rf current at the hairpin was estimated to be 1.7 gauss per ampere.

For reasons of convenience the light source was kept outside the apparatus, and the light was focused onto the beam with a cylindrical lens of 2 in. focal length placed directly over the portion of the beam in the hairpin. The main object of the optical system was to focus the wide light source onto the relatively narrow beam. With some of the lamps a cylindrical reflector was placed above the lamp to reflect additional light into the apparatus. With this optical system the optical

⁹ J. M. B. Kellogg and S. Millman, *Revs. Modern Phys.* **18**, 323 (1946).

illumination in the hairpin was about 1/20 of the surface brightness of the lamp. A shutter was used between the light source and the apparatus to turn the light beam on and off. The light source itself will be discussed in Sec. 3.d.

b. The Production and Measurement of the rf Current

Two oscillators were used to continuously cover the rf frequency range of 6 Mc/sec to 240 Mc/sec, and to produce up to 3 amp of rf current at the hairpin. The range from 6 to 100 Mc/sec was covered by a tuned plate, tuned grid, push-pull, triode oscillator using lumped impedance tuned circuits. The transmission line from the hairpin was conductively coupled to the plate coil. The range of 100 to 240 Mc/sec was covered with a tuned plate, tuned cathode, push-pull, triode oscillator using tuned lines for the resonant circuits. The transmission line from the hairpin was inductively coupled to the plate circuit and was also tuned to obtain sufficiently high currents in the hairpin. Regulated power supplies were used for the B voltages and continuously charged storage batteries were used for the filament supplies of both oscillators.

The transmission line from the oscillators to the hairpin was a parallel plate line, with the same characteristic impedance as the hairpin would have if the shorts were removed from the end of the hairpin. The magnetic field in the hairpin was determined by measuring the rf current in the transmission line at a fixed distance from the hairpin and calculating the rf current at the hairpin from the usual transmission line equations. The transmission line equations were experimentally found to hold for the structure used in this experiment. For frequencies below 60 Mc/sec, the transmission line current was measured with an rf ammeter of the thermocouple type. For frequencies above 60 Mc/sec a special probe was constructed, which used a loop to pick up the magnetic field inside the transmission line and a crystal to rectify the induced current. The probe was absolutely calibrated at low frequency using the rf ammeter, and the probe readings projected to higher frequencies using the theoretical behavior of the loop and crystal with frequency.

As shown by Torrey,⁷ the magnitude of the rf magnetic field determines the width of a ground state resonance if the field is much greater than the optimum field. The rf fields used in this experiment were of this size and therefore the width of the ground state ($2, -2$) to ($2, -1$) rf resonance was used to measure the rf field. The frequency of the resonance was varied over the frequency range of the experiment by increasing the static magnetic field, and the resonance width for a constant rf current was measured. By doing this we were able to show that the probe, with the theoretical

corrections for its frequency behavior, was a good measure of the rf magnetic field in the hairpin.

c. The Detection System

In the early stages of the experiment the conventional atomic beam surface ionization detection system was used. With this equipment the $3^2P_{3/2}$ state resonances were first found, but the signal-to-noise ratio was very bad since the excited state rf effects were only 8×10^{-5} of the total beam and had to be read on top of the light effect which was 2×10^{-2} of the total beam.

Therefore a modulated rf detection system was introduced which increased the rate of taking data by about a factor of ten and at the same time considerably increased the accuracy of the data. This design was copied in large part from the detection system devised by R. T. Daly at the Massachusetts Institute of Technology. The basic idea of the method is shown schematically in Fig. 1. The rf oscillators are square-wave modulated at 34 cps, in order to have a modulation frequency which is not a harmonic or subharmonic of 60 cps. The modulation of the oscillators produces a square-wave-modulated rf magnetic field, which induces a square-wave-modulated rf effect on the unmodulated background of the light effect and fast atoms. The beam is ionized on a hot tungsten ribbon. The ions leaving the detector pass through a simple mass spectrometer which removes noise producing impurity ions introduced by the hot wire. The principal impurity as shown by the spectrometer is potassium. The ions are then further accelerated onto the first plate of an Allen-type electron multiplier whose output is fed into a tuned amplifier. The output of the amplifier, which consists only of the modulated portion of the signal due to the rf effect, is rectified in a lock-in circuit. The rectified signal is averaged in a long time constant RC circuit and fed into a Speedomax recorder.

The main components of the detection system will now be discussed in more detail. A Hewlett Packard audio oscillator is used to generate the basic 34-cps signal for the rf modulation. The audio signal is amplified in order to drive a Western Electric Mercury Relay 275C which is biased with a dc current so as to produce square-wave operation of the relay. A negative voltage sufficient to cut off the oscillator tubes is put through the relay onto the grids of the oscillator tubes. In this way the oscillators are square-wave modulated and produce a modulated rf field.

The portion of the beam which has been affected by the rf is square-wave modulated when it leaves the C -field region, but the velocity distribution of the atoms in the beam demodulates the rf effect as the atoms travel away from the hairpin. At 34 cps the demodulation is negligible in our apparatus when the beam hits the detector ribbon. However, in some cases the demodulation may set an upper limit to the modulation frequency which can be used in an atomic beam

apparatus. Another possible source of demodulation is the time required for an alkali atom to evaporate from a hot tungsten surface after impinging on the surface. This "sitting" time depends upon the temperature of the tungsten and about 1200°C was necessary in our case to reduce the "sitting" time of sodium to below 0.001 sec. To ionize the sodium the tungsten surface had to be kept oxidized and this was done in the conventional way with a very small stream of oxygen continuously falling on the tungsten surface. The minimum "sitting" time which can be attained was not determined, but this may constitute another limit on the maximum modulation frequency.

The ionizing system and mass spectrometer are shown in Fig. 1. The spectrometer uses permanent magnets, and the focusing is accomplished by changing the accelerating potential. The magnetic field of the spectrometer is of circular cross section and produced by two cylindrical Alnico magnets inside a steel pipe which acts as both a return path for the flux and as a magnetic shield. While the use of a circular cross section prevents high-order focusing, it makes the adjustment of the spectrometer easy and uncritical. The spectrometer is placed in the beam path so that the neutral beam passes through the spectrometer before reaching the detector ribbon. The ions leaving the detector ribbon then return along the path of the neutral beam until they enter the spectrometer, where they bend through an angle of 60 degrees in order to leave through the exit slit. The spectrometer is the equivalent of a 60-degree sector magnet with a radius of 3.0 cm. The detector ribbon is 0.010 in. wide and the accelerating slit is 0.040 in. wide. The accelerating slit is grounded while the guard plate and detector ribbon are at a positive voltage. The collecting efficiency of the ionizing system is improved by putting a small negative potential on the ribbon with respect to the guard plate, which for sodium was about 6 volts. The exit slit, which is also grounded, serves as the selecting aperture and is also 0.040 in. wide. The slit positions are all adjusted before the spectrometer is placed into the system, since no internal mechanical adjustments can be made on the spectrometer in vacuum. The product of the required focusing voltage and the atomic number is 8000 volts and the resolution is about 100 percent of the mass number being focused. The overall efficiency of the ionizer and spectrometer is 15 to 20 percent. Since the ionization itself is almost 100 percent efficient, these losses are in the accelerating slit and spectrometer proper. Such losses are not unusual in a spectrometer of this type.

When the ions leave the spectrometer they are accelerated by another 0.040 in. wide slit onto the first plate of the Allen tube. This second accelerating slit is electrically connected to the first plate of the Allen tube so that the ions are accelerated through the full voltage of the tube which is 3500 to 4500 volts.

The tube has 16 beryllium copper dynodes supported in mica side-plates. Ordinary 1.2-Meg carbon resistors are connected from each dynode to the adjacent ones to serve as voltage dividers. The resistors were placed in the vacuum system without harming the resistors or the vacuum. The tube was first activated by following the procedure recommended by Allen, but later it was found that one could activate by simply cleaning and carefully polishing the dynodes. This gave an initial gain of 1 000 000 which, while not as high as the gains obtained by Allen, was sufficient for our purposes. In a period of about 3 months, the gain decreased to about 10 000 and the tube was reactivated. The ionizing system, mass spectrometer, and the Allen tube are all mounted from a single movable support, so that when the detector ribbon is moved for line up purposes, the entire assembly moves together.

The three-stage tuned amplifier used on the output of the Allen tube has a gain of 300 and a band width of 6 cps which is attained by a twin-tee feedback loop from the third to the first stage. Another Western Electric Mercury Relay 275C is used for the lock-in circuit rectifying switch, and is driven from the same audio signal which drives the rf modulating relay. To adjust for phase shifts in the detection system, the amplifier which drives the lock-in relay has a phasing circuit. The lock-in relay is also biased with a dc current so as to act as a square-wave rectifying switch. The *RC* averaging circuit has a variable time-constant but is usually run with a 20-sec time constant. The averaged signal from the *RC* circuit passes through a set of high-impedance variable attenuators into a cathode follower which matches the high impedance of the attenuators into the low-input impedance of the recorder.

For line-up purposes and light-effect measurement it is necessary to measure the steady-output current of the Allen tube. This is done by using a vacuum tube voltmeter to read the voltage produced by the Allen tube across a high resistance. The short time-constant of the voltmeter makes line-up procedure much faster than with the usual long-time-constant galvanometer system.

d. Light Sources

The requirements on the light source are that the emitted light have a high intensity at the desired wavelength, that the lamp have a low noise level, and that the lamp operate uniformly for long periods. The probability for excitation of the atoms is proportional to the intensity of that portion of the resonance radiation whose frequency falls within the absorption width of the atomic beam. Since the atoms in the beam do not undergo collisions and since the Doppler effect is negligible, the absorption width of the atoms is just the natural width. Therefore the beam absorbs radiation only from a very small region about the center of the emission line of the lamp. The lamp must be designed and operated so as to have a maximum intensity at the

center of the spectral line and so that self-reversal is minimized.

For this experiment the General Electric NA-1 and the Philips SO 60 W sodium arc discharge lamps were used. If the G.E. lamp is used as directed by the manufacturer, the $^2S_{1/2}$ to $^2P_{3/2}$ spectral line is badly self-reversed as measured by a Fabry-Perot. The light effect was increased and the self-reversal decreased by running the lamp without a vacuum jacket, with 3-amp ac through each filament, and with 3-amp dc arc current. The dc arc current was obtained from the 110-volt dc line using 33 ohms for ballast. In this way about 8 percent of the atoms were excited. The Philips SO 60 W lamp was run from the specified ballast transformer but without a vacuum jacket, and under these conditions the arc current was 0.7 amp. The Philips lamp gave a maximum of 16 percent excited atoms. The Philips sodium spectral lamp 93122 was also tried and found to be about as effective as the G.E. lamp. These three types of lamps proved to be more effective than others of our own construction.

The second requirement on the light source is a low noise level. The noise level of the lamps was studied by observing the increase in noise output of the detection system when the light effect was being measured. The root-mean-square noise due to light effect was about 0.0001 of the magnitude of the light effect for the commercial arc discharge lamps, when observed with a 20-sec time-constant. These commercial lamps also met the third requirement of long-term stability. Over periods of a day the intensity would change by only a few percent, a change for which the data could easily be corrected.

4. PROCEDURE

a. The Method of Taking Data

The C field was set at the desired static magnetic field by measuring the frequency of the $(2, -1)$ to $(2, -2)$ rf transition in the ground state. The minimum C field which was used was $\frac{1}{2}$ gauss. Smaller C fields gave nonadiabatic transitions because of the fringe fields from the A and B magnets which overlapped into the ends of the C magnet. The resonance lamp was adjusted to give maximum light effect with no attempt being made to distinguish between light effect due to the $3^2P_{3/2}$ state and light effect due to the $3^2P_{1/2}$ state. In some cases the lamp was unusually noisy and some compromise had to be reached between the quietness of the operation and the magnitude of the light effect.

The procedure for taking data was complicated by the ground state transition $(2, -1)$ to $(2, -2)$. When runs were made at small magnetic fields, this ground state transition occurred at frequencies of the order of 1 Mc/sec, and if rf near this frequency was used to study the excited state, this ground state transition occurred in addition to the excited state rf transition. As the rf frequency (f) is moved away from the center of the ground state transition (f_0), the intensity of the

ground state rf effect decreased as $[(f-f_0)^2+d^2]^{-1}$, where d is the half-width at half-intensity of the ground state resonance. The ground state resonance therefore had a long tail, and even at relatively high frequencies some ground state rf effect occurred. In data taken at small magnetic fields, the ground state rf effect was about equal to the excited state rf effect at 30 Mc/sec and was about $\frac{1}{10}$ the excited state rf effect at 60 Mc/sec. It is possible to design an apparatus in which no ground state rf effect will be observed when the excited state rf effect is measured. To distinguish between the ground state and excited state rf effects it was necessary to measure the rf effect when the beam was optically excited and again when the beam was not optically excited. The first measurement gave the sum of the excited state and ground state rf effects, while the second measurement gave only the ground state rf effect. The difference of these two measurements was the excited state rf effect.

To measure the excited state rf effect, the oscillator was set to the desired frequency and desired rf current. The light shutter was opened so that the beam was optically excited and a timing circuit was started. This circuit first allowed a 1-minute "wait" time for the averaging circuit to reach equilibrium. The timing circuit then turned on the recorder for 40 sec during which time the recorder read the total rf effect, that is, the excited rf effect plus ground state rf effect. This gave a trace about 4 in. long on the recorder which would be a straight line if there were no noise. When the 40-sec reading time was finished, the light shutter was closed so that the beam was no longer optically excited, and the timing circuit was started again. After the one-minute "wait" time, the recorder read the ground state rf effect alone for 40 sec. It is to be noted that the oscillators were on, and being modulated continuously, throughout the readings. This incidentally helped to keep the oscillators stable. For each frequency this procedure of reading total rf effect and ground state rf effect was repeated several times. When the data at one frequency were completed, the oscillator was tuned to a new frequency and adjusted to give the same rf current. In this way the oscillator frequency was moved across the frequency range of interest. The procedure of point-by-point data-taking had to be adopted because of the need to keep the rf current constant, which was more important in this experiment than in the usual ground state experiments.

The rf current in the hairpin was measured by the rf ammeter and rf probe described in Sec. 3.b. During the run the C field was measured several times using the frequency of the $(2, -1)$ to $(2, -2)$ ground state transition, and the field was readjusted when necessary. The magnitude of the light effect was also measured frequently since changes of the order of 10 to 20 percent were found to occur over the course of a run, mainly because of changes in the total beam rather than in the

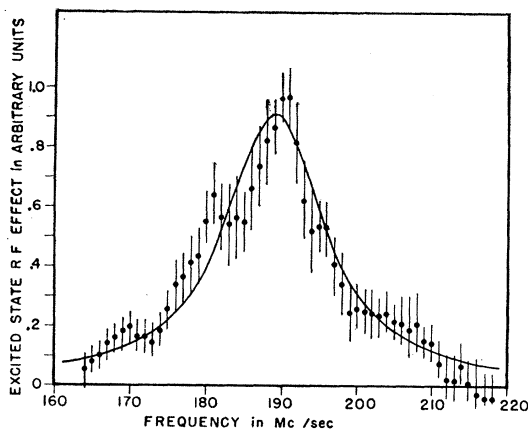


FIG. 5. A typical resonance curve for the 3^2P_1 state taken at 2.0 gauss static field and 2.8 amp rf. The dots with vertical probable error lines are the experimental points. The curve is a "best fit" of the simple resonance formula, Eq. (2), to the experimental points.

light intensity. The data for an excited state spectrum were generally acquired by going over the spectrum four times in one run to make sure there were no apparatus drifts. The final data usually consisted of three or four pairs of total rf effect and ground state rf effect measurements at half-megacycle intervals. An average straight line was drawn through each trace by eye and the rf effect corresponding to this line was taken as the average rf effect for that trace. The difference of these average values of the total rf effect and the ground state rf effect in each pair was the excited state rf effect for that pair. These excited state rf effect measurements are the raw data of the experiment.

The excited rf effect was easily corrected for any drifts in the light effect. When the ground state rf effect was very large, there was another simple correction because the light effect and ground state rf effect cancelled each other to a small extent.

b. Fitting of the Data

The corrected excited state rf effect plotted against the rf frequency gave the rf spectrum of the excited state with some scatter of the points due to various sources of noise. For interpretation and fitting of the data, it was found useful to plot an average spectrum made up by taking the average of all the points in the interval of a megacycle, giving average points which were averages of 6 to 8 independent measurements. The averaging over 1-Mc/sec intervals is legitimate because the spectra are made up of resonances each of which has approximately a 20-Mc/sec width.

The interpretation of the experimental curves is more important in this experiment than in the usual ground state experiment because the resonances widths are of the same order of magnitude as the level separations. If a single rf transition is induced between two

excited state hyperfine levels, and interference terms and rf level perturbations are neglected, then the form of the excited state rf resonance will be

$$I = h / [(f - f_0)^2 + g^2], \quad (2)$$

according to the theory in Appendix 2. Here I is the intensity of the resonance, h is the height, g is the half-width at half-intensity, f_0 is the center of the resonance, and f is the rf frequency. The weak-field excited resonances $\Delta F = \pm 1$, $\Delta m_F = \pm 1, 0$ consist of a number of almost superimposed transitions between the Zeeman levels of the two F states. The superposition is not perfect because the static and rf magnetic fields perturb the levels. The individual resonances are shifted only a small amount compared to their width, and not as much as the individual Zeeman levels. We therefore still use a curve of the form of Eq. (2) to fit the total resonance. One may expect that there will be some fine structure at the peak of the total resonance and that the width of the total resonance will be slightly greater than the natural width. In fitting the weak-field spectra, Eq. (2) was used with more emphasis given to the sides of the observed resonance than to the top. No attempt was made to make the highest point on the resonance coincide with the center of the resonance. There is some uncertainty in this type of fitting, which leads to errors independent of the signal-to-noise ratio. However the experimental conditions do not warrant a more detailed study.

5. RESULTS

The rf spectra were studied from 6 to 240 Mc/sec at static magnetic fields of about 1 gauss. A single resonance was found at the higher end of this range, Fig. 5. The resonance is asymmetric so that the peak is at a higher frequency than the center when determined by fitting a curve of the form of Eq. (2). The average value of the center is 188.9 Mc/sec. This resonance was studied at rf currents of 1.4 to 3.2 amp and static fields of 1.0 to 2.0 gauss.

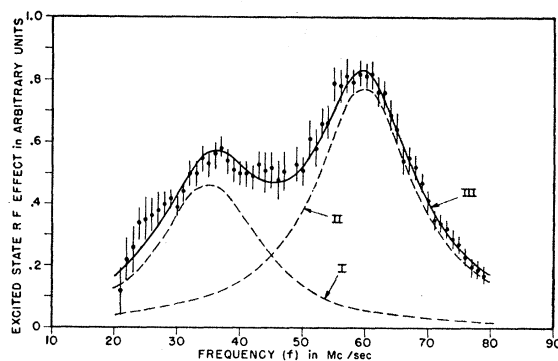


FIG. 6. A typical resonance curve for the 3^2P_1 state taken at 1.84 gauss static field and 1.4 amp rf. The dots with the vertical probable error lines are the experimental points. Curves I and II are the individual resonance curves and curve III is their sum. The parameters of the curves are chosen to give a "best fit" of curve III to the experimental points.

A much stronger excited state spectrum was found in the lower frequency range and a typical curve taken at 1.4 amp rf and 1.84 gauss static field is shown in Fig. 6. All of the experimental curves which are shown in this paper have arbitrary intensity units and no direct comparison in intensity should be made between different figures. This stronger spectrum was explained, as will be discussed later, as being the sum of two overlapping resonance curves arising from transitions in the $3^2P_{3/2}$ state. The parameters of the individual resonances were derived by fitting the experimental points to an expression of the form

$$I = \frac{h_I}{(f_I - f)^2 + g^2} + \frac{h_{II}}{(f_{II} - f)^2 + g^2}, \quad (3)$$

where the subscripts I and II refer to the lower and upper individual resonances respectively which make up the total curve. In this expression h_I and h_{II} are relative heights of the two resonances, f_I and f_{II} are the centers of the two resonances, and g is the width of the individual resonances which includes the broadening produced by the rf and static magnetic fields in addition to their natural width. g is the same for both resonances because the lifetimes of all of the hyperfine states in the same fine-structure state are the same. The fitting of Eq. (3) to the experimental points was done by trial and the best fit was estimated by eye. The parameters obtained in five different runs with this type of fitting are given in Table I.

Figure 7 shows a spectrum taken at 60.8-gauss static field and 2.8-amp rf current which was used in the evaluation of b . Spectra were obtained at a number of other values of the static field, but they are not of direct interest in the evaluation of b and are not presented in this paper.

6. DISCUSSION OF RESULTS

a. Assignment of Resonances

If a light filter is interposed in the optical system which filters out the sodium "D" line, the excited state rf resonances described in the last section all disappear. Therefore these resonances may definitely be assigned to the $3^2P_{3/2}$ and $3^2P_{1/2}$ states of Na²³. We next assign the 188.9-Mc/sec resonance to the $F=2$ to $F=1$ transition in the $3^2P_{3/2}$ state in agreement with the optical measure-

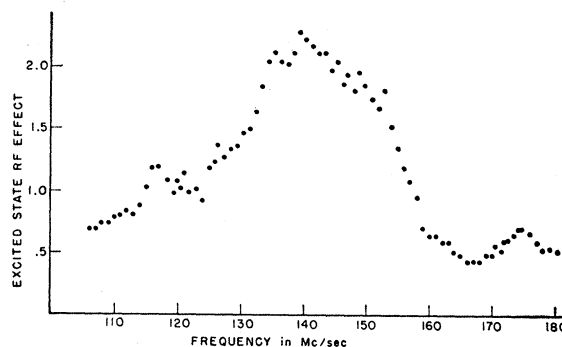


Fig. 7. The Paschen-Back spectrum of the $3^2P_{3/2}$ state taken at 60.8 gauss static field and 2.8 amp rf. The dots are the experimental points.

ment of Jackson and Kuhn¹⁰ of 192 ± 10 Mc/sec. This assignment is also confirmed by the calculation of this separation from the Landé equation¹¹ relating the hyperfine separation to the fine structure separation, which predicts the value of 186 Mc/sec if 8.0 is used for Z_i . Since this hyperfine separation is equal to $2a_3$, the experimental value of a_3 is 94.45 Mc/sec.

The two lower resonances are now assigned to the $3^2P_{3/2}$ state. The zero-field separations of the F levels in the $3^2P_{3/2}$ state are given in Eq. (1). Ideally one would expect to find three resonances for this state, but simplified intensity calculations indicate that the $F=1$ to $F=0$ resonance may be very weak. The possible assignments of the two observed resonances can be restricted by using the information obtained in the $3^2P_{1/2}$ state. According to the simple theory¹¹ of the magnetic hyperfine structure constants, the ratio of $a_{3/2}/a_{3/2}$ is 5. Therefore a_3 must be 18.9 Mc/sec within a few percent.¹² From Eq. (1) and Table I we can calculate all the possible experimental values of a_3 . The assignment of the two overlapping resonances to the $F=3$ to $F=2$ transition and $F=2$ to $F=1$ transition leads to an a_3 of 19.06 Mc/sec in agreement with the prediction. All other assignments give values of a_3 which are at least 25 percent different from the predicted value. Therefore the two observed resonances are assigned to the 3-2 and 2-1 transitions, with the value of a_3 taken as 19.06 Mc/sec.

The final assignment problem is whether to assign the upper resonance to the 3-2 transition and the lower resonance to the 2-1 transition or to make the converse assignment. The value of a_3 is independent of how this final assignment is made but the value of b is not. The two possible assignments with the corresponding values of b and the position of the 1-0 resonances are listed in

TABLE I. Parameters obtained by fitting the weak-field $3^2P_{3/2}$ spectrum in five different runs.

f_I , center of lower peak in Mc/sec	f_{II} , center of upper peak in Mc/sec	g , half-width in Mc/sec
35.0	58.5	9.75
35.5	59.8	9.80
35.4	59.8	9.80
36.0	60.2	9.75
35.8	60.5	9.90

¹⁰ D. A. Jackson and H. Kuhn, Proc. Roy. Soc. (London) **167**, 205 (1938).

¹¹ H. Kopfermann, *Kernmomente* (Edwards Brothers, Inc., Ann Arbor, 1945), p. 22.

¹² Davis, Feld, Zabel, and Zacharias, Phys. Rev. **76**, 1076 (1949), discussed the accuracy of this theory and found for light elements such as Al²⁷ that the ratio is correct to within a few percent.

TABLE II. Assignment of the $3^2P_{\frac{3}{2}}$ weak-field resonances for the two possible values of b .

b in Mc/sec	Frequency of $F=3$ to $F=2$ in Mc/sec	Frequency of $F=2$ to $F=1$ in Mc/sec	Frequency of $F=1$ to $F=0$ in Mc/sec
+ 2.58	59.8	35.5	16.5
- 21.64	35.5	59.8	40.7

Table II. If the 1-0 resonance lies at 40.7 Mc/sec, it is not surprising that it was not observed because calculations indicate that the intensity of the 1-0 resonance is $\frac{1}{10}$ to $\frac{1}{5}$ of the intensity of the 2-1 resonance, and the fitting is not sufficiently accurate to disclose a small peak between two large peaks. The other possible position of the 1-0 resonance is 16.5 Mc/sec, but in the present apparatus the signal-to-noise ratio is low at this frequency because of the presence of a large ground state effect. Therefore we have not been able to determine whether or not a peak exists at 16.5 Mc/sec.

Another way in which resonances can be identified is by the comparison of theoretical and experimental intensity ratios as is done in optical spectroscopy. At weak magnetic fields, the presence of large interference terms makes the calculation of the relative intensities of the excited state rf resonances very sensitive to the magnitudes and directions of the static and oscillating magnetic fields. These quantities were not sufficiently well known in our experiment to enable us to make a trustworthy calculation.

However, a more reliable calculation of the intensity of the excited state rf effect can be made for strong fields when the excited hyperfine states are well separated. Twelve transitions are allowed with the selection rules $\Delta m_J = \pm 1$ and $\Delta m_I = 0$. The calculation of their relative intensities shows that the transition ($m_J = \frac{1}{2}$, $m_I = \frac{3}{2}$) to ($m_J = -\frac{1}{2}$, $m_I = \frac{3}{2}$) results in an excited state rf effect which is about nine times larger than the effect due to any of the other transitions. Fig. 7, which shows the Paschen-Back spectrum of the state, has one large peak with a center at about 144 Mc/sec. From the known magnetic field of 60.8 gauss, the frequency of the ($\frac{1}{2}, \frac{3}{2}$) to ($-\frac{1}{2}, \frac{3}{2}$) transition is 142.4 Mc/sec for $b = +2.58$ Mc/sec and is 148.9 Mc/sec for $b = -21.64$ Mc/sec. To better compare the experimental peak with the two possible calculated frequencies, the backgrounds due to the other $3^2P_{\frac{3}{2}}$ transitions and to a $3^2P_{\frac{1}{2}}$ transition were subtracted from the experimental curve. The net result is shown in Fig. 8. The two curves refer to the two possible b values since the background also depends on the value of b . For $b = +2.58$ Mc/sec, the experimental peak center is 142 ± 1 Mc/sec and the calculated center is 142.4 Mc/sec, while for $b = -21.6$ Mc/sec the experimental center is 140 ± 1 Mc/sec and the calculated center is 148.9 Mc/sec. Thus, the Paschen-Back spectrum of the $3^2P_{\frac{3}{2}}$ state can best be explained by the value $b = +2.58$ Mc/sec if the strong resonance is due to the ($\frac{1}{2}, \frac{3}{2}$) to ($-\frac{1}{2}, \frac{3}{2}$) transition. This spectrum

is therefore a strong indication for selection of $b = +2.58$ Mc/sec, but we do not feel that it is a positive proof for this selection. We therefore use both values of b in evaluating the nuclear quadrupole moment.

The strong resonance in the Paschen-Back spectrum, Fig. 8, does not have the shape of the simple resonance curve of Eq. (2), but is wider and has a flat top. The explanation for this shape lies in the fact that the electron angular momentum $J = \frac{3}{2}$ is largely decoupled from the nuclear spin and that the three separations between the four successive energy levels are equal to within the line width. The transitions are therefore more like the transitions which can be made by a system with a magnetic moment and with a spin of $\frac{3}{2}$ in an external magnetic field, where one resonant frequency can cause transitions from each m_J level to every other m_J level. The transition probabilities were calculated from the formula first given by Majorana.¹³ From the approximate value of the oscillating magnetic field the theoretical resonance curve was calculated and found to agree quite well with the experimental resonance shape. This was additional confirmation of our interpretation of the Paschen-Back spectrum of the $3^2P_{\frac{3}{2}}$ state.

b. Discussion of the Limits of Error

In setting the limits of error on the experimental values of $a_{\frac{3}{2}}$, $a_{\frac{1}{2}}$, and b , one must consider the possible errors produced by the small static magnetic field. The static fields were sufficiently small in all the runs that the effect of quadratic Zeeman shifts of the levels on the three constants is negligible. However if the intensities of the excited state rf effects produced by various Zeeman transitions between the same two F levels vary greatly, it is possible for the resonances and the constants to shift linearly with changes in the magnitude of the static field. However, there was no evidence of such shifts taking place in either the $3^2P_{\frac{3}{2}}$ or $3^2P_{\frac{1}{2}}$ state.

The fitting procedure must also be considered in setting the limits of error. Because of the asymmetry in the 188.9-Mc/sec resonance, we have taken the value of the hyperfine separation in the $3^2P_{\frac{3}{2}}$ state as 188.9 ± 1.0 Mc/sec, where the ± 1.0 -Mc/sec error is the limit to which the center can be shifted while maintaining a reasonable fit in all the measurements of this resonance. This gives the value

$$a_{\frac{3}{2}} = 94.45 \pm 0.5 \text{ Mc/sec.}$$

Each experimental spectrum for the $3^2P_{\frac{3}{2}}$ state at small magnetic field was fitted separately and the fitting parameters are listed in Table I. Because of this independent fitting the average values of $a_{\frac{3}{2}}$ and b must be calculated in the following way. For each of the runs the $a_{\frac{3}{2}}$ and b are calculated, and the averages of these five independent measurements of these con-

¹³ F. Bloch and I. I. Rabi, Revs. Modern Phys. 17, 237 (1945).

stants is taken as the average value of the constants. Now the divergencies between the individual values of the constants are due in part to the problem of fitting. Since this type of error is difficult to evaluate statistically, we take the limits of experimental error on the constants as the maximum divergence of the individual values of the constants from the average values of the constants. The limits of error on the constants will be larger if peaks from different runs are used to evaluate them. This is because each fit was done independently and some of the fittings give higher values of the peak frequencies than others. When the entire fitting curve is shifted up, this has a larger effect on $a_{\frac{3}{2}}$ than it has on b because b depends mainly on the difference of the peaks while $a_{\frac{3}{2}}$ depends on the sum of the peaks. We can then give the value

$$a_{\frac{3}{2}} = 19.06 \pm 0.36 \text{ Mc/sec,}$$

where the errors include the evaluation of $a_{\frac{3}{2}}$ from peaks belonging to different runs. For b , we have the choice of the two values:

$$b = +2.58 \pm 0.18 \text{ Mc/sec,}$$

$$b = -21.64 \pm 0.54 \text{ Mc/sec,}$$

where the limits of error are only for the calculation of b from peaks belonging to the same run. To include

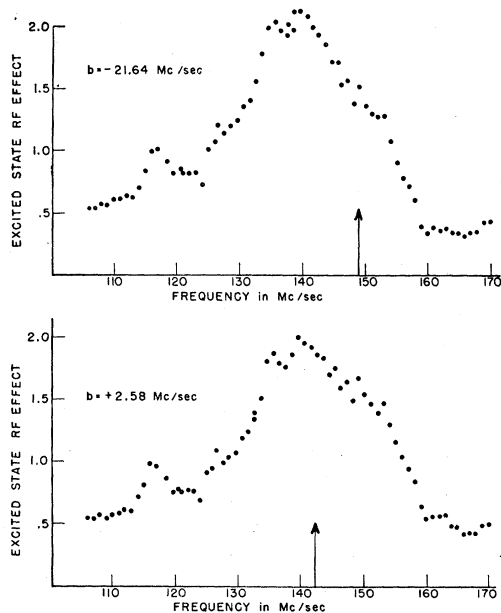


FIG. 8. A comparison of the Paschen-Back spectrum of the $3^2P_{\frac{3}{2}}$ state at 60.8 gauss with the calculated position of the $(\frac{3}{2}, \frac{3}{2})$ to $(-\frac{1}{2}, \frac{3}{2})$ transition. The spectrum is shown with the background due to all other transitions subtracted out for the two possible values of b , since the background depends on the value of b . The vertical arrow in each graph is the calculated position of the $(\frac{3}{2}, \frac{3}{2})$ to $(-\frac{1}{2}, \frac{3}{2})$ transition for the value of b indicated on the graph. For $b = +2.58$ Mc/sec the agreement of the experimental center with the calculated center is much better than for $b = -21.64$ Mc/sec.

TABLE III. Experimental ratios of the excited state rf effect to the light effect^a at the center of the excited state rf resonance.

State	Center of resonance in Mc/sec	Static magnetic field in gauss	Rf current in amp	Intensity rf effect / Intensity light effect ^a
$3^2P_{\frac{3}{2}}$	59.8	1 to 2	1.4	0.0040
$3^2P_{\frac{3}{2}}$	35.5	1 to 2	1.4	0.0024
$3^2P_{\frac{3}{2}}$	142	60.8	2.8	0.0043
$3^2P_{\frac{3}{2}}$	188.9	1 to 2	2.8	0.0008
$3^2P_{\frac{3}{2}}$	188.9	1 to 2	1.4	0.0002

^a The light effect is the total light effect due both to the $3^2P_{\frac{3}{2}}$ and $3^2P_{\frac{1}{2}}$ states. For the lamps used in this experiment, the ratio of the light effect due to the $3^2P_{\frac{1}{2}}$ state to the light effect due to the $3^2P_{\frac{3}{2}}$ state was about 2.

the values of b obtained by using peaks from different runs, and to allow for any possible undetected shifts due to the static magnetic field, we have increased the limits of error for the two possible values of b as follows:

$$b = +2.58 \pm 0.3 \text{ Mc/sec,}$$

$$b = -21.64 \pm 0.7 \text{ Mc/sec.}$$

These results agree with those given by Sagalyn,³ which were 19.5 ± 0.6 Mc/sec for $a_{\frac{3}{2}}$ and 2.4 ± 1.4 Mc/sec for b .

c. Experimental Line Shapes and Intensities

The observed widths of the $3^2P_{\frac{3}{2}}$ resonances which are given in Table I must be corrected for the broadening effect of the rf and static magnetic fields. If this is done, the average corrected natural half-width is 9.56 ± 0.2 Mc/sec. The lifetime of the $3^2P_{\frac{3}{2}}$ state from this natural width is $(1.66 \pm 0.04) \times 10^{-8}$ sec. The corrected natural half-width of the $3^2P_{\frac{1}{2}}$ resonance is 8.0 ± 1.0 Mc/sec, giving a lifetime for the $3^2P_{\frac{1}{2}}$ state of $(2.0 \pm 0.25) \times 10^{-8}$ sec. Stephenson¹⁴ found the lifetime of both of these states to be $(1.61 \pm 0.06) \times 10^{-8}$ sec by using a different method.

At weak magnetic fields the ratio of the light effect to the total beam was 0.02 to 0.04 depending on the type of lamp. When the field was increased to several hundred gauss the light effect increased about 75 percent in agreement with theoretical light effect calculations. The ratio of the intensity of the excited state rf effect to the light effect is given in Table III for several cases the ratio could only be compared with theory for the strong field $3^2P_{\frac{3}{2}}$ resonance where we could make a reliable calculation. Making use of the Majorana formula as described at the end of Sec. 6.a, the ratio calculated from the approximate value of the rf field agreed with the experimental ratio within the error introduced by the uncertainty of the proportion of the experimental light effect due only to the $3^2P_{\frac{3}{2}}$ state.

7. CONCLUSIONS

The results of the experiments on the $3^2P_{\frac{3}{2}}$ and $3^2P_{\frac{1}{2}}$ states show that within the range of our experimental

¹⁴ G. Stephenson, Proc. Phys. Soc. (London) A64, 458 (1951).

error, the ratio of a_1/a_3 is 5.0 in agreement with simple theory.

The value of b is related to the nuclear electric quadrupole moment Q by the well known relation

$$b = -e^2 Q \langle 3 \cos^2 \theta - 1 \rangle_{Av} \langle r^{-3} \rangle_{Av}, \quad (4)$$

where θ and r are the coordinates of the valence electron. The value of $\langle r^{-3} \rangle_{Av}$ can be found from the known nuclear magnetic moment of Na^{23} (μ_I), and from a_1 or a_3 . If the deformation of the electronic core by the valence electron is neglected, the equation for Q becomes

$$Q = \frac{b \mu_0 \mu_I (l+1)(2l+3)}{a_j e^2 (I)(j)(j+1)}, \quad (5)$$

where μ_0 is the Bohr magneton and e is the electronic charge. The values of Q calculated from Eq. (4) are

$$\begin{aligned} b &= +2.58 \pm 0.3 \text{ Mc/sec}, & Q &= +0.108 \pm 0.012 \times 10^{-24} \text{ cm}^2, \\ b &= -21.64 \pm 0.7 \text{ Mc/sec}, & Q &= -0.909 \pm 0.030 \times 10^{-24} \text{ cm}^2, \end{aligned}$$

where the limit of error on Q are due only to the errors in b and a .

Sternheimer has shown in a number of papers¹⁵ that the electron core may result in a shielding or an anti-shielding of the quadrupole moment, and that the observed quadrupole moment will then be smaller or larger, respectively, than the true quadrupole moment. There is also an analogous effect in the magnetic dipole interaction constant, and both of these effects are calculated together because of certain cancellations which occur. Therefore the correction for Q is given as a correction for the ratio of b/a_3 . For the $3^2P_{3/2}$ state of Na^{23} , Sternheimer has made a specific calculation and finds that the true value of Q is equal to 0.92 of the observed value of Q . Therefore the values of Q which are given above must be multiplied by 0.92 giving the following corrected values of Q :

$$\begin{aligned} b &= +2.58 \pm 0.3 \text{ Mc/sec}, & Q &= +0.100 \pm 0.011 \times 10^{-24} \text{ cm}^2, \\ b &= -21.64 \pm 0.7 \text{ Mc/sec}, & Q &= -0.836 \pm 0.028 \times 10^{-24} \text{ cm}^2. \end{aligned}$$

The simple shell model predicts that the nucleus is in a configuration with a resultant Q of zero. Sengupta¹⁶ and Scharff¹⁷ have shown that by mixing configurations, positive values of Q can be obtained of the order of magnitude of the positive Q found in this experiment.

The atomic beam resonance method can be applied to excited states of atoms to yield results of interest despite the natural width of the resonance lines. With

an arrangement which allows the selection of a particular initial magnetic ground state, the signal to noise problem and the problem of identification of the transitions will be greatly simplified. At present the apparatus used in this experiment is being used to investigate the hyperfine structure of the excited states of Rb^{85} and Rb^{87} .

We wish to take this opportunity to acknowledge our debt to Professor P. Kusch, Dr. G. K. Woodgate, and Dr. Charles A. Lee who in large part constructed the first form of this apparatus with which the effects of optical and radiofrequency radiation in the excited state were first detected.

APPENDIX 1

a. General Equation for the Light Effect

Consider a static magnetic field in the z direction and a beam of unpolarized light which is propagated in the y direction. This is the situation in our experiment. (a) is used to designate the initial ground state of the atom, (b) and (b') are used to designate excited states of the atom, and (c) is used to designate the final ground state of the atom. The light beam can be considered to be made up of x polarized and z polarized light. $G(b, a, x)$ is the electric dipole transition matrix element for a transition from the ground state (a) to the excited state (b) induced by x polarized light. Similarly $G(b, a, z)$ is the electric dipole transition matrix element for light polarized in the z direction. In considering the decay process it is only necessary to take account of spontaneous emission. The electric dipole transition matrix element for decay from the excited state (b) to the final ground state (c) with emission of light polarized in the x direction is $G(c, b, x')$. Similarly $G(c, b, y')$ and $G(c, b, z')$ are the electric dipole transition matrix elements for decay with emission of y -polarized and z -polarized light respectively. The relative probability, $W(c, a)$, of an atom going from an initial ground state (a) to a final ground state (c) is

$$\begin{aligned} W(c, a) &= \sum_{p=x, z} \sum_{p'=x', y', z'} \\ &\times \left[\sum_b (|G(c, b, p')|^2 |G(b, a, p)|^2) + \sum_{b, b'; b \neq b'} \right. \\ &\left. \times \left(\frac{G(c, b, p') G(b, a, p) G(c, b', p')^* G(b', a, p)^*}{1 + 4\pi^2 T^2 [f(b, b')]^2} \right) \right], \quad (6) \end{aligned}$$

where T is the lifetime of the excited state in seconds and $f(b, b')$ is the separation of the excited states (b) and (b') in cycles per second.

The relative light effect due to atoms originally in the ground state (a) is

$$L(a) = \sum_c W(c, a), \quad (7)$$

¹⁵ R. Sternheimer, Phys. Rev. **84**, 244 (1951); **86**, 316 (1952); and **95**, 736 (1954).

¹⁶ S. Sengupta, Phys. Rev. **96**, 235 (1954).

¹⁷ M. F. Scharff, Phys. Rev. **95**, 1114 (1954).

where the summation is over all of the final states (c') which have a value of m_J different from the m_J value of the initial ground state (a).

The relative light effect due to all atoms is obtained by summing $L(a)$ over all of the initial states taking into account the relative populations of the initial states. If a substantial portion of the atoms are excited twice, then the light effect produced by the second excitation must be calculated from the ground state populations which resulted from the first excitation. In our experiment, the magnetic hyperfine ground states are equally populated initially. Also, the probability of an atom being excited more than once is very small so that the light effect due to second excitations can be neglected. Therefore in our experiment the total relative light effect is

$$L = \sum_a L(a), \quad (8)$$

where the summation is over all of the initial states (a).

The ratio of the total light effect to the number of atoms which have been optically excited is R_L , where

$$R_L = L / [\sum_c W(c, a)] \quad (9)$$

and the summation is over all initial and final states. The probability, P , that an atom is optically excited depends on the intensity of the radiation and the time that the atoms spend in the illuminated region. The ratio of the light effect to the total beam is the product PR_L .

In Eq. (6) the first term gives the transition probability if all interference effects are neglected. The second term contains the interference effects and its importance depends on the magnitude of $Tf(b, b')$. If the excited state levels are widely separated with respect to their width which is $(2\pi T)^{-1}$, then $Tf(b, b')$ is large and the interference term can be neglected. In the excited states of Na²³ the interference term cannot be neglected in general, and the complete calculation of the variation of the light effect with magnetic field is tedious. However, there are two cases in which the calculations can be simplified, and these cases will now be discussed.

b. Light Effect at Zero Magnetic Field

At zero magnetic field the excited state (b) is designated by the quantum numbers (F, m_F) where F and m_F have their usual meaning. At zero field all of the m_F levels in a single F level are degenerate. The interference terms between m_F levels in different F levels can be neglected with an error of less than 10 percent for the $3^2P_{3/2}$ and $3^2P_{1/2}$ states of Na²³. With this approximation Eq. (6) reduces to

$$W(c, a) = \sum_{p=x, z} \sum_{p'=x', y', z'} \sum_F \sum_{m_F} |G(c; F, m_F; p') G(F, m_F; a; p)|^2. \quad (10)$$

From Eq. (10), R_L is 0.22 for the $3^2P_{3/2}$ state and 0.40 for the $3^2P_{1/2}$ state. R_L may be thought of as the ratio of the light effect to the total beam if each atom is optically excited once and only once.

c. Light Effect at Strong Magnetic Field

At strong magnetic fields in which I and J are decoupled in the excited states, the levels are sufficiently separated to allow the interference term to be neglected with an error of less than 10 percent in the $3^2P_{3/2}$ and $3^2P_{1/2}$ states of Na²³. For convenience we define

$$D(c, b) = \sum_{p'=x', y', z'} |G(c, b, p')|^2, \quad (11)$$

$$E(b, a) = \sum_{p=x, z} |G(b, a, p)|^2.$$

If the second term in Eq. (6) is neglected, we obtain

$$W(c, a) = \sum_b D(c, b) E(b, a). \quad (12)$$

From Eq. (12), R_L is 0.36 for the $3^2P_{3/2}$ state and 0.41 for the $3^2P_{1/2}$ state.

APPENDIX 2

We shall derive an equation for the excited state rf effect due to an rf transition between two excited states (b) and (b'), and neglect interference effects and rf perturbation of the levels. The probability $s(b, b')$ of making an rf transition from the state (b) to the state (b') in a time t is given by the equation

$$s(b, b') = \frac{V^2 \sin^2\{\pi t [V^2 + (f - f_0)^2]\}}{V^2 + (f - f_0)^2}, \quad (13)$$

where V is the rf matrix element and f_0 is the frequency separation of the levels (b) and (b'); both of these quantities are in units of cps. The average value, $S(b, b')$, is obtained by integrating $s(b, b')$ with the probability that an excited state lasts for a time t which is $\exp(-t/T)$. T is the lifetime of the excited state. The value of $S(b, b')$ is

$$S(b, b') = \frac{V^2}{2[V^2 + k^2 + (f - f_0)^2]}, \quad (14)$$

where $k = [2\pi T]^{-1}$.

We can use the light-effect theory of Sec. C of Appendix 1 for this discussion because we are neglecting interference effects. Taking account of only those atoms which come from the ground state (a), the population of the excited state (b) is $E(b, a)$ and of the excited state (b') is $E(b', a)$, if no rf is applied. When the rf is applied, the population of (b) is decreased by the probability that an atom makes an rf transition to (b') which is $S(b, b')$. The population of (b) at the same time is increased by an amount $[S(b', b)][E(b', a)]$,

since $S(b',b)$ is the probability for an atom to make an rf transition from (b') to (b) . When the rf is applied the population of (b) is changed to

$$[1-S(b,b')][E(b,a)]+[S(b',b)][E(b',a)]. \quad (15)$$

A similar expression holds for the population of (b') . $D(b,c)$ is the probability of an atom decaying from (b) to a final ground state (c) . Therefore the change in $W(c,a)$ produced by the rf is $\Delta W(c,a)$, where

$$\Delta W(c,a) = \{[D(c,b)][-E(b,a)+E(b',a)] + [D(c,b')][-E(b',a)+E(b,a)]\} \{S(b,b')\}, \quad (16)$$

and we have used $S(b,b')=S(b',b)$. Equation (16) reduces to

$$\Delta W(c,a) = [D(c,b)-D(c,b')][E(b',a)-E(b,a)] \times \left[\frac{V^2}{2[V^2+G^2+(f-f_0)^2]} \right]. \quad (17)$$

The total relative excited state rf effect ΔW is

$$\Delta W = \sum_{c'} a W(c,a), \quad (18)$$

where the summation is over all initial states (a) and those final states (c') which have a value of m_J which is different from the m_J value of the initial state (a) . This is the same type of summation as the one described in Sec. A of Appendix 1 in the calculation of the total relative light effect. The ratio of the excited state rf effect to the light effect, which is the quantity of experimental interest, is simply $(\Delta W)/L$.

Equation (17) shows that ΔW depends on the optical matrix elements connecting (b) and (b') to the ground state levels. It is this dependence which leads to wide variation in the intensities of the excited state rf effects between different pairs of excited state levels. From Eq. (14), the width of the excited state rf effect resonance curve at half-intensity is g , where

$$g^2 = k^2 + V^2. \quad (19)$$

Photoprotons from Lead-208 and Tantalum*

M. ELAINE TOMS† AND WILLIAM E. STEPHENS

Physics Department, University of Pennsylvania, Philadelphia, Pennsylvania

(Received December 23, 1954)

The photoprotons ejected from thin foils of tantalum and enriched lead-208 by the 23-Mev bremsstrahlung x-rays from a betatron have been observed in nuclear emulsions. Yields, measured in units of 10^4 protons per mole per roentgen unit, are: tantalum, 5.6 ± 0.5 ; lead-208, 2.6 ± 0.3 . The angular distribution of the lead-208 protons shows a strong forward asymmetry while the tantalum protons are more isotropic. Both proton energy distributions are in good agreement with the predictions of the direct photoprocess.

PREVIOUS work^{1,2} has shown that the Coulomb barrier in heavy elements ($Z > 40$) strongly inhibits the emission of "evaporated" photo protons. Many of the photoprotons that are observed are ascribed to a direct photoeffect.^{1,3} We have extended these measurements to the photoprotons from tantalum and lead enriched in isotope 208.⁴

Using the techniques described previously,^{1,5-7} Ilford E-1 200-micron plates were placed in an evacuated "camera" to detect charged particles ejected from thin foils by collimated x-rays from the University of Pennsylvania betatron run at 23 Mev. The plates were de-

veloped by the temperature change method and later scanned. The track ranges were corrected by adding half the effective foil thickness and converted to photon energies. Table I gives the details of the two runs.

The energy distributions of the photoprotons are shown in Figs. 1 and 2. The tracks between 2 and 5

TABLE I. Exposure details.

	Tantalum	Lead-208
Foil thickness (mg/cm ²)	16.6	21.8
(mils)	0.4	0.75
Effective half-thickness for 10-Mev protons (Mev)	0.16	0.2
Purity	0.99+	0.966
X-ray exposure (roentgens)	28 950	27 850
Area scanned (cm ²)	2.1	2.2
Protons measured	414	231
Alphas observed	2	2
Estimated proton background	40±16	44±16
Proton tracks observed in background region (2-5 Mev)	20	20
Yields:		
(10 ⁴ protons mole ⁻¹ roentgen ⁻¹)	5.6±0.5	2.6±0.3
(10 ⁴ alphas mole ⁻¹ roentgen ⁻¹)	0.003±0.02	0.04±0.03

* Supported in part by the joint program of the Office of Naval Research and the U. S. Atomic Energy Commission.

† Now at the Naval Research Laboratory, Washington, D. C.

¹ M. E. Toms and W. E. Stephens, Phys. Rev. **92**, 362 (1953).

² E. V. Weinstock and J. Halpern, Phys. Rev. **94**, 1651 (1954).

³ E. D. Courant, Phys. Rev. **82**, 703 (1951).

⁴ We are indebted to the Isotopes Division of the U. S. Atomic Energy Commission for the loan of the enriched lead.

⁵ M. E. Toms and W. E. Stephens, Phys. Rev. **82**, 709 (1951).

⁶ P. R. Byerly and W. E. Stephens, Phys. Rev. **83**, 54 (1951).

⁷ M. E. Toms and W. E. Stephens, Phys. Rev. **95**, 629(A) (1954).